A new method for manufacturing dry electrodes on textiles. Validation for wearable ECG monitoring

Josué Ferri [a], Raúl Llinares [b],[*], Izan Segarra [c], Antonio Cebriánv [c], Eduardo Garcia-Breijo [e], José Millet [c],[d]

[a] *Textile Research Institute (AITEX), 03801 Alicante, Spain*
[b] *Departamento de Comunicaciones, Universitat Politècnica de València, 03801 Alcoy, Spain*
[c] *ITACA Institute, Universitat Politècnica de València, Valencia, Spain*
[d] *CIBER CV, Madrid, Spain*
[e] *Instituto Interuniversitario de Investigación de Reconocimiento Molecular y Desarrollo Tecnológico (IDM), Universitat Politècnica de València, Universitat de València, 46022 Valencia, Spain*

A B S T R A C T

This paper presents a new dry ECG electrode printed on a textile substrate. The proposed manufacturing process permits cost-effective mass production. The ECG dry electrode is obtained through screen printing a conductive silver ink coated with a biocompatible carbon layer. Three different designs combining two shapes (circular and square) and two sizes were developed. The resulting measured impedances are similar to those obtained via a conventional electrode. The prototypes were attached to a bracelet and used with a commercial electrocardiogram (ECG) device to register ECG signals. The dry electrodes were validated via ECG monitoring and compared with a conventional wet electrode. The clinical interest intervals reported similar results and the QRS morphology presented slight differences. Noise evaluation showed no notable differences for all the analyzed parameters.

1. Introduction

Health monitoring and its associated electronics have attracted considerable interest from the scientific community in recent years. The electrocardiogram (ECG) is the most common method to assess and diagnose cardiovascular diseases [1]. Ambulatory electrocardiography (AECG) involves continuous ECG monitoring on an outpatient with a Holter monitor device, while the patient goes about their daily activities. Traditional uses of AECG for arrhythmia detection have broadened as the result of increased use of multichannel, telemetered signals and computation. Current AECG equipment provides for the detection and analysis of arrhythmias and ST-segment deviation, as well as more sophisticated analyses of R-R intervals, QRS-T morphology including late potentials, Q-T dispersion and T-wave alternans [2].

Wearable devices have become an active part of health monitoring. They enable continuous monitoring of health parameters, opening up endless possibilities. Wearables can also contribute to algorithm development for the prediction, prevention and intervention of diseases [3]. In the field of cardiac health, since wearables can obtain long recordings of an acceptable quality, they can adopt different types of analysis used in AECG monitoring.

The most common types of noise in ECG signal acquisition are baseline wander (BW), power line interference (PLI) and muscle artefacts (MA). In some cases, a contaminated ECG beat can hinder subsequent quality analysis. Noise mostly results from BW, as this type of noise can be caused by respiration, body movement, poor electrode contact or skin-electrode impedance [4]. The frequency spectrum of BW ranges from 0.05 to 1 Hz, although in the case of respiration, the range is between 0.15 and 0.3 Hz. MA noise is located in higher frequencies (around 150 Hz). Noise in ECG measurements represents about 10% of the ECG amplitude, generally with a bandwidth of between 20 and 1000 Hz [5].

Conventional ECG/AECG systems use silver/silver chloride (Ag/AgCl) electrodes to register ECG signals. This type of electrode uses a gel that functions as an electrolyte to decrease skin–electrode impedance. This gel can produce skin irritation, allergic reactions or itchiness. In addition, it can dry out during long recordings, potentially provoking changes in signal quality.

To overcome these challenges, researchers have developed dry electrodes that function without the need for any kind of gel [6]. One group of these dry ECG solutions is based on smart textiles. This kind of ECG electrode can be integrated into textiles, thereby offering a more

* Corresponding author at: Escola Politècnica Superior d'Alcoi, Plaça Ferrándiz i Carbonell, s/n, 03801 Alcoi, Alacant, Spain.
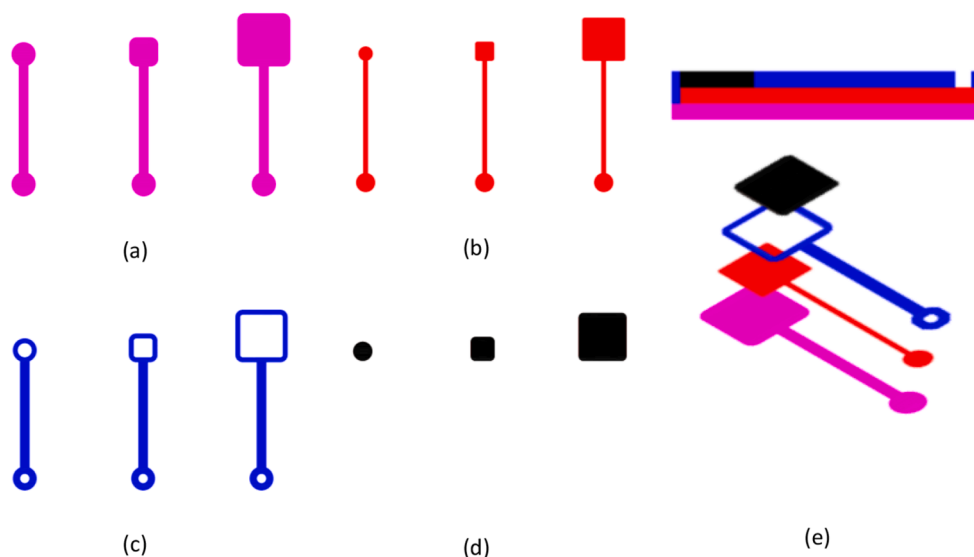*E-mail address:* rllinares@dcom.upv.es (R. Llinares).

Fig. 1. Parts of the multilayer printed electrode for the three designs: (a) Insulating material to protect the electrode layer and prevent the electrode from coming into contact with the adhesive; (b) Electrode and track printed with a silver conductive ink; (c) Insulating material to prevent the conductive track from coming into contact with the skin; (d) Protection of the electrode made with carbon ink; (e) 3D layout of the electrode showing the different layers.

comfortable solution, since they do not need to adhere to the skin and, as they are integrated into the textiles, offer properties such as breathability, flexibility and stretchability.

Smart textile ECG electrodes can be obtained by integrating conductive fibers or threads during the manufacturing process through weaving [7] or knitting [8]. Other approaches use electronic printing [9], where conductive inks are deposited on the textile substrate and the electrode is integrated on the substrate. Several printed electrode solutions can be found, depending on the conductive material used. Some of them use silver ink [10] to make up the electrode, due to good conductivity and ease of printing. However, most metallic inks are based on nanoparticles that present certain health risks, making them unsuitable for contact with the skin [11]. Recently, research has been conducted using carbon as the conductive material due to its biocompatibility. In [12], a carbon-based electrode is proposed, entailing lower conductivity due to the nature of carbon. Other studies have successfully selected carbon nanostructures such as graphene [13] or carbon nanotubes [14]. Although these solutions show very promising results, they still have high production costs. Other promising printed electrode techniques, not related to smart textiles, include tattooing methods [15]. In this case, the main challenge is the electronic conditioning of the signal, which can prove less reliable and robust [16].

One of the main challenges of textile ECG electrodes is the manufacturing process in terms of cost and mass production. Manufacturing that involves weaving or knitting has certain limitations when it comes to creating electrodes with identical dimensions. Moreover, they must be positioned correctly for each garment and size. These conditions usually lead to high costs, especially for mass production. The manufacturing process using electronic printing presents some limitations because, to maintain reasonable costs, printing must be applied before making the garment. This requires precise positioning of the electrodes when cutting out the fabric after tracing the patterns prior to assembly.

This article presents and evaluates a new dry textile electrode design that also allows for an alternative manufacturing solution. On the one hand, the electrode is screen-printed using a high conductivity material, silver ink, which is combined with a biocompatible carbon layer to protect the subject's skin. On the other hand, the proposed method involves an initial printing of the electrode on a plastic or paper substrate that is subsequently transferred to the textile by applying heat. This allows the electrodes to be attached in a certain position even after the

garment has been made. More importantly, the proposed solution can be applied to different fabrics or garments, facilitating manufacturing in the value chain. The design has been evaluated using ECG recordings from 10 subjects and compared to those produced by high-end, off-the-shelf disposable gelled Ag/AgCl electrodes. The results are reported in terms of the most common intervals in AECG, waveform morphology and noise content.

2. Materials and methods

2.1. Materials

Polyamide/Lycra knitted fabrics with a weight of 140 g/m^2 and a thickness of 0.5 mm were used. This textile was selected to offer some stability whilst maintaining elasticity. The elastic property enables the application of enough force for the electrodes to come into contact with the skin at the right pressure. Dycotec DM-SIP-2001 ink with a high silver content was selected for printing the electrodes. This ink offers a solid content of between 66% and 73% and a stretchability performance of up to 140% on most substrates. This ink is used in general electronic printing applications and presents stretchable properties suitable for wearables. CAP-4301 carbon ink was used to encapsulate the silver electrode and prevent it from coming into direct contact with the skin. Finally, an encapsulating ink was used as insulation to protect the conductive ink. The ink is Dycotec DM-ENC-2500 which has suitable properties for wearable and medical devices. This ink paste is appropriate for textile printing due to its elastomeric properties and stretchability. In addition, a thermo-adhesive layer was applied to permit adhesion to the textile. Finally, a metal snap connector was placed on the textile electrode to connect it to the leads of an ECG recording module.

2.2. Fabrication methods

2.2.1. Design of the electrode

The electrode is composed of four layers. The first layer insulates the electrode from the adhesive. The second layer is a highly conductive material, silver ink, which facilitates the electrode function, as well as the connection with the snap connector. The third layer consists of an insulating ink that prevents the electrode track from coming into contact with the skin. And finally, a material deposited on the conductive

Table 1

Dimensions of the different designs and the conventional Ag/AgCl ECG electrode.

Shape	Radio / Side Length	Area (mm²)	Image
CE	$R = 4$ mm	50.26 mm²	
SE	$L = 10$ mm	96.57 mm²	
BSE	$L = 20$ mm	396.57 mm²	
RE	$R = 5.01$ mm	79 mm²	

electrode comprises the fourth layer. This material, a carbon ink, is less conductive than the first, but ensures good contact with the skin. Fig. 1 shows the arrangement of each of the printed layers.

Three electrode designs with different shapes (circular and square) and sizes were considered to evaluate the behavior of the ECG electrode. Table 1 shows the dimensions of the different designs. The electrodes are denoted CE (Circular), SE (Square), BSE (Big Square) and RE (Reference Ag/AgCl). The corners of the squares are rounded, thereby reducing the surface area.

2.2.2. Printing

The screen-printing method was selected due to its cost and versatility. It offers a wide range of ink types compared to other printing methods such as inkjet or flexography. In addition, this technique uses inks with a high viscosity that allows a thick layer deposition, ensuring the stability of the printed material, as well as high conductivity. The printing was carried out on a temporary plastic substrate that fulfils two functions. Firstly, it permits homogeneous printing due to the uniformity of the surface, overcoming problems derived from printing directly onto the textile, such as loss of conductivity due to the thickness or roughness of the textile [17]. Secondly, it is suitable for transferring the electrode to a fabric by heat-sealing. All the inks were gently stirred following the manufacturer's instructions in order to ensure good dispersion and always avoiding the formation of bubbles. The printed samples were cured at 140 °C for 30 min in an oven.

2.2.3. Heat-sealing

The heat-sealing process enables the transfer of a print located on a temporary substrate onto a textile. To this end, a final layer of adhesive was applied after the printing process. The electrode was placed on the fabric before heat and pressure were applied to transfer it onto the fabric. This way the print adheres to the fabric and subsequently the transfer material is removed. For this transfer, 150 °C of heat and 10 bars of pressure were applied for 10 s.

2.2.4. Bracelet manufacturing

Once the electrodes were placed on the textile using a heat-sealing technique, a snap-type button was attached. These snaps are made of brass, a conductive alloy of copper and zinc. The brass snap used is nickel-plated to ensure durability and protection against oxidation. This connector is subsequently used to connect the measurement equipment. The design incorporates a pigtail track to avoid any force derived from the connector that could affect electrode performance. Finally, a double fabric bracelet was manufactured using a conventional sewing process to test the electrodes. The electrodes are located in the inner tissue, while the snaps to connect the measurement equipment remain on the outside. The bracelet also incorporates a velcro-type fabric so that it can be adjusted to the dimensions of the arm or wrist to be placed where needed. Fig. 2 shows the prototype.
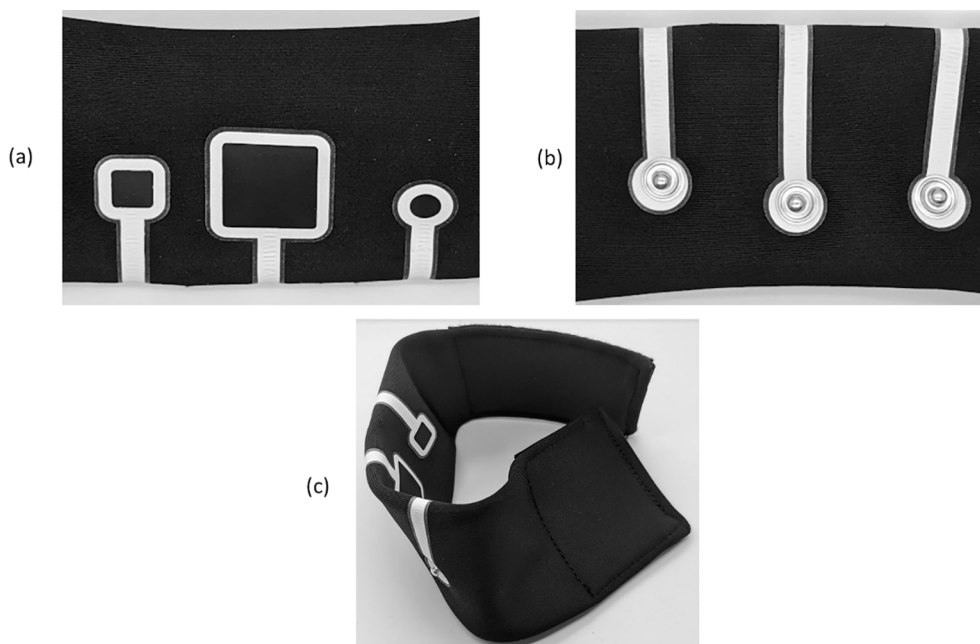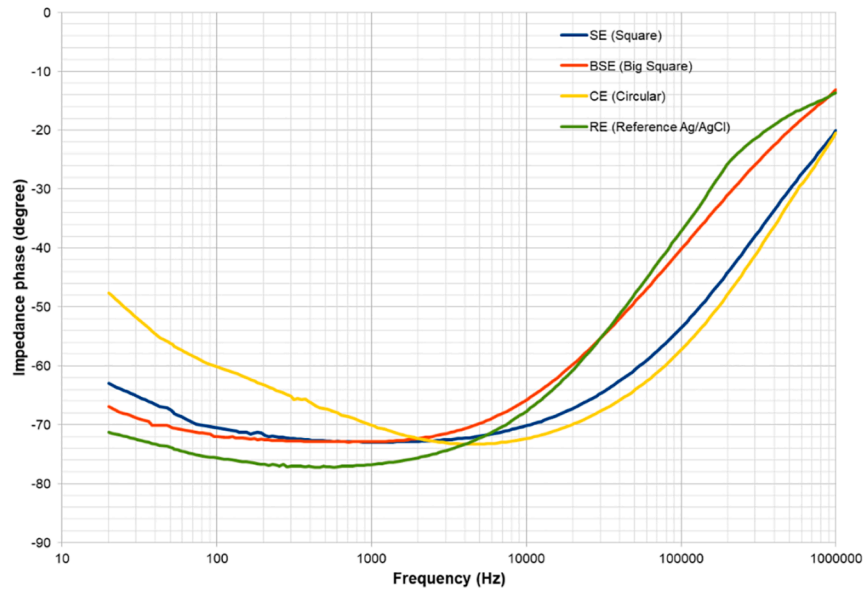

Fig. 2. Detail of the bracelet. (a) inner layer; (b) outer layer; (c) bracelet form.
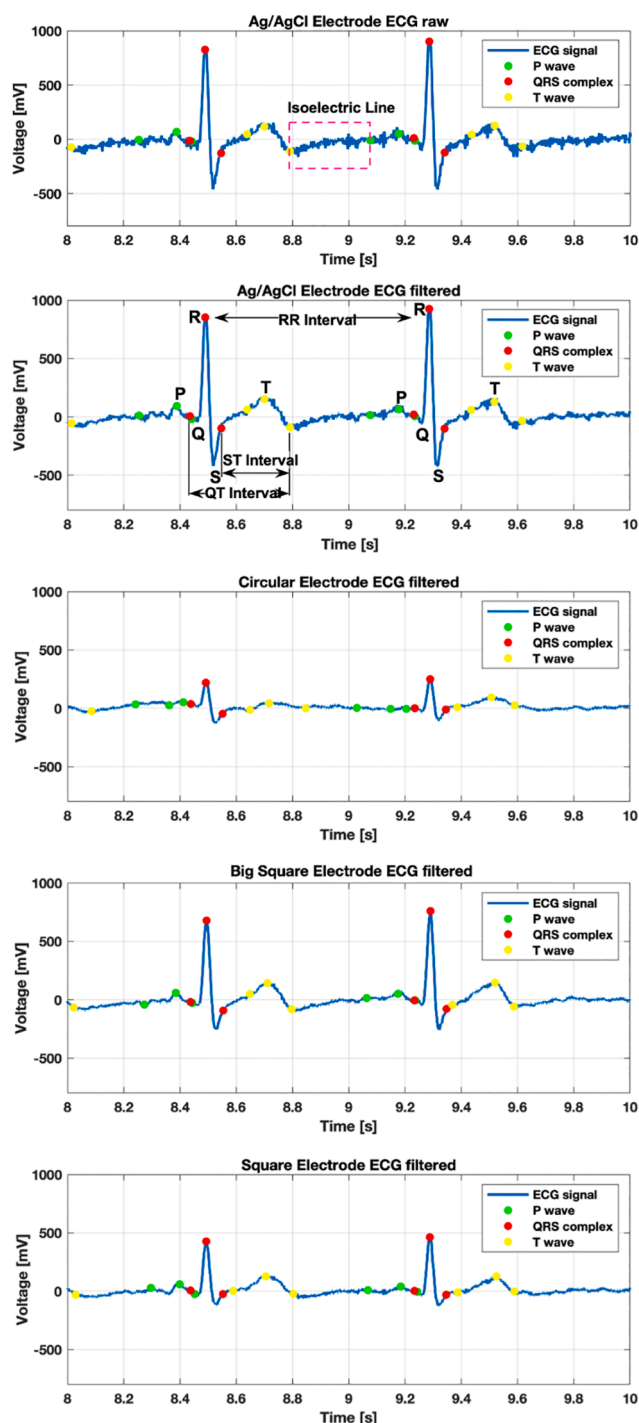
(a)
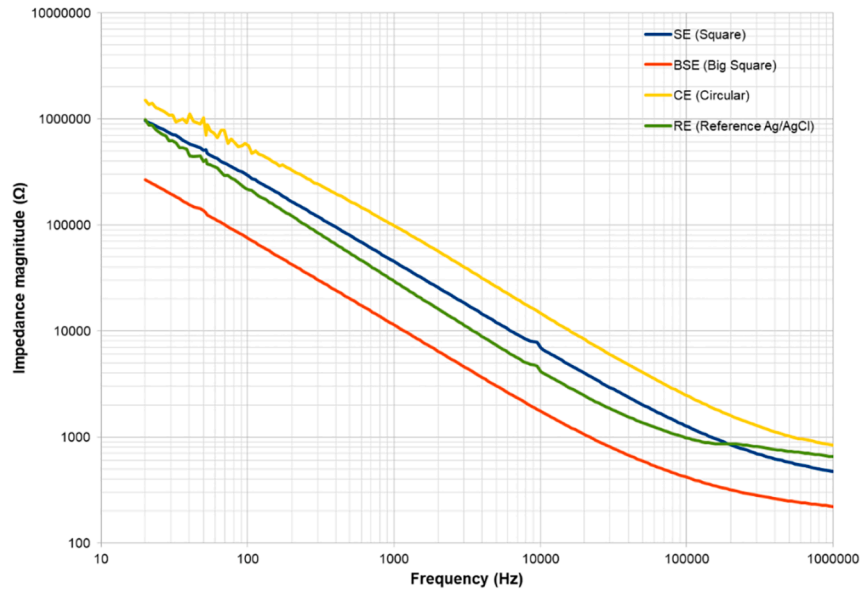
(b)

(c)

Fig. 3. (a) Location of the bracelets on the forearm for electrode characterization; Impedance measurements for the proposed dry ECG electrodes and RE: (b) magnitude (c) phase.

Fig. 4. One subject recording for all the electrodes (QRS fiducial points in red, P waves in green and T waves in yellow). The TP segment used in the analysis is shown in a pink dotted window. RR, QT and ST intervals are indicated using black arrows. (For interpretation of the references to colour in this figure legend, the reader is referred to the web version of this article.)

2.3. Measurement methods

2.3.1. Electrical conductivity measurements

Textile electrode impedance was measured and compared with medical grade Ag/AgCl wet electrodes (Ambu WhiteSensor WS 00 S/ 50). To determine the ECG electrode impedance, a frequency sweep from 20 Hz to 1 MHz was carried out with a LCD meter (BK PRECISION model 895). For these measures, the ECG electrodes were located on the

forearm at a distance of 10 cm apart (Fig. 3a).

2.3.2. Signal acquisition

Ten voluntary healthy participants gave their informed consent (eight male and two female, age: 23 ± 2 years). Five recordings were made for each subject. Four of them corresponded to sequential recordings using the four electrodes. The last recording was a simultaneous register of the four electrodes. The signals were acquired for periods of 10 s by means of a pair of disposable gelled Ag/AgCl electrodes (White Sensor WS-00-S, Ambu) and two bracelets with the three proposed textile electrodes on each one. The electrodes were located close together on the right arm (RA) and on the left arm (LA). In all cases, the recording corresponded to Lead I (LA – RA) of the standard ECG. The total recording time was 1 h and 10 min, with each subject taking approximately 7 min.

Differential electrical signals were amplified (x200) and band filtered between 0.1 Hz a 100 Hz (-6 dB) using a Grass amplifier (CP511 AC amplifier, Grass Instruments. Signals were digitized at 1 kHz using a multifunction Data Acquisition System from National Instruments (NI USB-6008 DAQ). The recordings were simultaneously acquired using an ECG standard recording system developed in our laboratory.

2.3.3. ECG signal processing

In order to obtain many of the intervals and other features described in the Introduction section, the first step was the estimation of the fiducial points from the ECG. For the data to be more reliable, some digital pre-processing of the ECG was performed, consisting of a band-pass filter and isoline correction. All processing was done using the open source toolbox "ECGdeli" from MATLAB [18].

Once the fiducial points were obtained, the next step was the estimation of the most representative intervals used in clinical practice: RR, QT and ST for each of the 10 s recordings (Fig. 4). Next, a morphological analysis of the QRS complex was carried out, as commonly applied in AECG analysis. In this case, the Pearson correlation coefficient (ρ) of two adjacent QRS complexes was estimated.

2.3.4. ECG noise evaluation

To estimate the effect of the noise, the TP segment was chosen as the isoelectric interval as it is the longest and most representative segment (pink dotted window in Fig. 4). The baseline was corrected using signal processing, implementing a median filter with partial overlapped windows, interpolating the values of the local median for each window.

The signal-to-noise ratio (SNR) was computed in order to evaluate the influence of noise in the acquired signals using the following formula:

$$SNR(dB) = 20log_{10}\left(\frac{V_{pp\_QRS}}{4\sigma_{noise}}\right) \qquad (1)$$

where V_{pp_QRS} corresponds to the peak-to-peak voltage obtained from the median of the maximum and minimum values of the QRS complex for each beat. The value σ_{noise} represents the median of the standard deviation of the noise corresponding to each isoelectric TP interval.

To determine the influence of BW and MA noises, a residual signal was obtained by subtracting the corresponding band-pass filtered ECG from the raw signal. In this way, all contributions below 0.67 Hz (BW) were included in the low-frequency analysis [19], whereas the ones corresponding to higher frequencies are mainly due to MA. The root-mean-square (RMS) value was also computed on each residual interval.

Finally, a frequency domain analysis was carried out. The power spectral density (PSD) of the residual signal was computed using a Welch periodogram (50% overlapped). The ratio of power corresponding to the most characteristic interval of the BW noise (PSD[0–0.67 Hz]/PSD$_T$) as well as that of the MA noise (PSD[60–150 Hz]/PSD$_T$) were estimated.

(a)

(a)

(b)
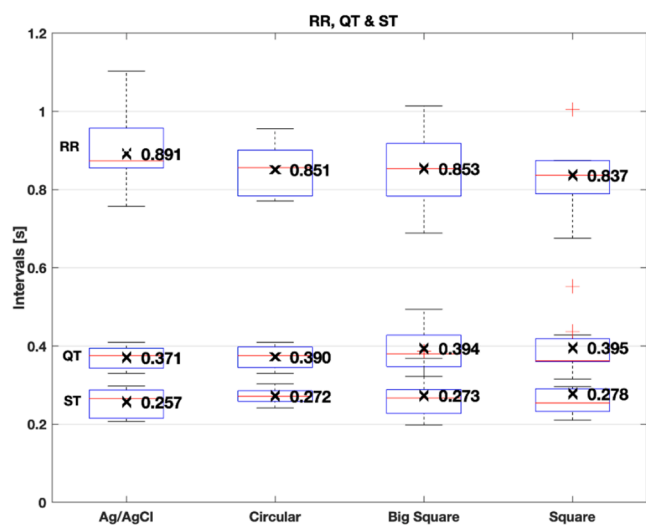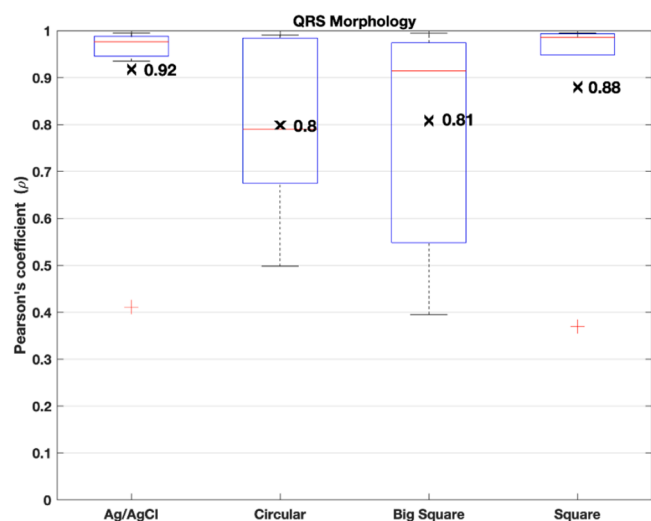
(b)

Fig. 5. (a) Box plot of the RR, QT and ST intervals for the 10 subjects. (b) Box plot of the intra-beat correlation of the 10 subjects. × corresponds to the average values.
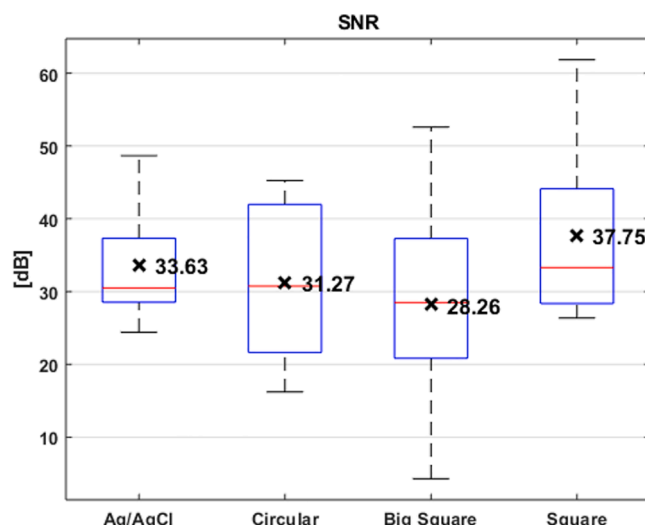
Fig. 6. For each electrode (a) SNR values. (b) RMS values of the low frequency content of the residual signal.

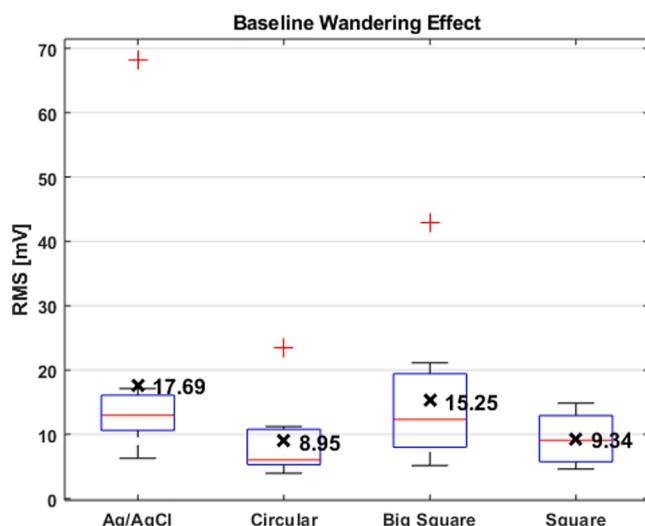## 3. Results

3.1. Electrode characterization

Impedance results (Fig. 3b and 3c) are consistent with electrode models [15], using the traditional Cole model to represent the skin and a resistor followed by a capacitor to represent electrode resistivity and skin connection. As expected, a bigger electrode area provides lower impedance. Small square electrodes provide the nearest results in terms of impedance to the medical grade Ag/AgCl wet electrode.

3.2. ECG intervals and morphology comparison

Fig. 5a summarizes the values of the RR, QT and ST intervals for the 10 subjects using a Box Plot. Bearing in mind that recordings were taken sequentially (one electrode after the other), the results were as expected and the variability corresponds to typical inter-subject variance. The

mean and standard deviation of the difference between intervals for each dry electrode and RE is close to zero. For the simultaneous recordings, in the case of the RR-intervals, the differences between the RE electrode and each dry electrode are 0.017 ± 0.042, 0.038 ± 0.066 and 0.030 ± 0.052 (CE, BSE, SE). Therefore, all the electrodes are suitable for RR, QT and ST interval analysis after the application of the digital signal preprocessing. Fig. 5b shows the results of the Pearson correlation coefficient (ρ) of two adjacent QRS complexes. A high degree of correlation (median > 0.9) can be observed in all the electrodes except in CE. A high level of variability was found for CE and BSE due to those cases where the QRS complexes are different.
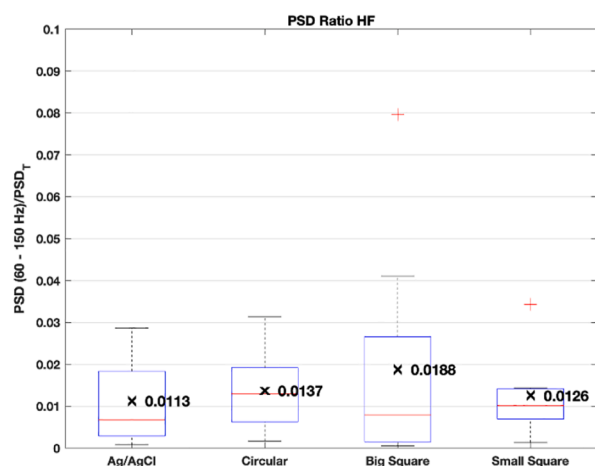
3.3. ECG noise evaluation

Fig. 6 shows that the median SNR values obtained are similar for the four types of electrodes (around 30 dB), whilst the variability is lower for RE. Although initially higher SNR values were expected for the big square (less impedance), the empirical results do not confirm this
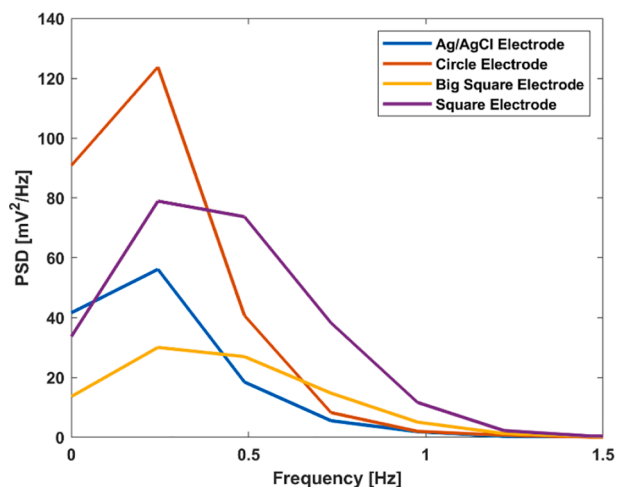
(a)
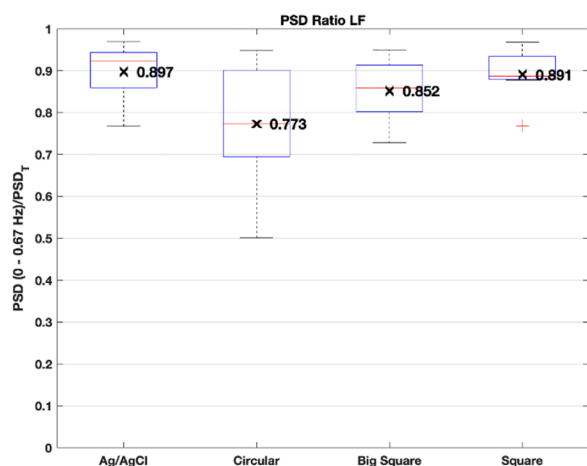
(b)

(c)

Fig. 7. (a) PSD (up to 1.5 Hz) for one of the subjects. (b) Power proportion for low frequencies (BW). (c) Power proportion for high frequencies (EMG).

assumption, possibly due to the observations made in [20], which noted that the electrode–skin impedance magnitude or phase is not sufficient to establish a relation with the SNR. With regard to the baseline artifact, the higher value corresponds to CE and the lowest to RE. The RMS values of the low frequency content of the residual signal are similar in all electrodes. Both small dry electrodes are around 9 mV.

Fig. 7a shows the low band PSD of the residual signal for a representative case. As can be observed, the BW noise contribution is higher for the small electrodes (CE is much higher than SE), while the lowest corresponds to BSE. With regard to the power ratios, for low frequencies (Fig. 7b), values are close to 1, even at such a small interval in comparison to the total, which shows that BW noise most affects ECG signals in controlled environments. Finally, Fig. 7c shows the effect of noise due to the MA. The values are close to zero and can thus be considered to be non-significant.

4. Conclusions

This study presents a new dry ECG electrode printed on a textile substrate. The electrode combines four layers to obtain a biocompatible dry solution. The upper layer, which comes into contact with the skin, contains a carbon coating that prevents the skin coming into direct contact with the silver ink, enabling the use of dry electrodes. With regard to the manufacturing process, the proposed method, based on thermo-sealing, permits the ECG electrode to be easily attached to any garment, enabling cost-effective mass production.

The proposed dry electrodes have been validated by comparing them with a conventional wet Ag/AgCl electrode. In terms of impedance, the results are as expected. Larger areas provide lower impedance values. With regard to the temporal ECG intervals, after applying conventional digital processing, the results are similar for all cases, especially in the case of RR intervals, one of the most commonly used intervals in clinical practice. The difference compared to the reference electrode is almost zero. In terms of the QRS morphology, although some variations are noticeable, the results are as expected, and a high correlation is found. With regard to noise evaluation, for all the analyzed parameters, there are no notable differences. The noise is concentrated on the low band and the lowest noise values are obtained for the big square electrode. It is possible to conclude that, for the static conditions of the study, any of the electrodes could be used. Future studies will look to analyze the influence of the contact of the electrodes and the behavior of the electrodes with subjects during their daily activities.

CRediT authorship contribution statement

Josué Ferri: Investigation, Methodology, Writing – original draft, Funding acquisition. **Raúl Llinares:** Investigation, Methodology, Writing – original draft, Project administration. **Izan Segarra:** Software, Data curation, Resources. **Antonio Cebriánv:** Conceptualization, Formal analysis, Data curation. **Eduardo Garcia-Breijo:** Investigation, Supervision. **José Millet:** Writing – original draft, Supervision, Funding acquisition, Project administration.

Declaration of Competing Interest

The authors declare that they have no known competing financial interests or personal relationships that could have appeared to influence the work reported in this paper.

(Instituto de Salud Carlos III)

References

[1] B.J. Drew, R.M. Califf, M. Funk, E.S. Kaufman, M.W. Krucoff, M.M. Laks, P. W. Macfarlane, C. Sommargren, S. Swiryn, G.F. Van Hare, Practice standards for electrocardiographic monitoring in hospital settings: An American Heart Association scientific statement from the councils on cardiovascular nursing, clinical cardiology, and cardiovascular disease in the young, Circulation 110 (17) (2004) 2721–2746, https://doi.org/10.1161/01.CIR.0000145144.56673.59.

[2] M.H. Crawford, S.J. Bernstein, P.C. Deedwania, J.P. DiMarco, K.J. Ferrick, A. Garson, L.A. Green, H.L. Greene, M.J. Silka, P.H. Stone, C.M. Tracy, R. J. Gibbons, J.S. Alpert, K.A. Eagle, T.J. Gardner, A. Garson, G. Gregoratos, R. O. Russell, T.J. Ryan, S.C. Smith, ACC/AHA guidelines for ambulatory electrocardiography: executive summary and recommendations: A report of the American College of Cardiology/American Heart Association Task Force on practice guidelines (Committee to Revise the Guidelines for Ambulatory El, Circulation 100 (8) (1999) 886–893, https://doi.org/10.1161/01.CIR.100.8.886.

[3] J. Dunn, R. Runge, M. Snyder, Wearables and the medical revolution, Per. Med. 15 (5) (2018) 429–448, https://doi.org/10.2217/pme-2018-0044.

[4] G.M. Friesen, T.C. Jannett, M.A. Jadallah, S.L. Yates, S.R. Quint, H.T. Nagle, A comparison of the noise sensitivity of nine QRS detection algorithms, IEEE Trans. Biomed. Eng. 37 (1990) 85–98, https://doi.org/10.1109/10.43620.

[5] U. Satija, B. Ramkumar, M. Sabarimalai Manikandan, A review of signal processing techniques for electrocardiogram signal quality assessment, IEEE Rev. Biomed. Eng. 11 (2018) 36–52, https://doi.org/10.1109/RBME.2018.2810957.

[6] A. Gruetzmann, S. Hansen, J. Müller, Novel dry electrodes for ECG monitoring, Physiol. Meas. 28 (11) (2007) 1375–1390, https://doi.org/10.1088/0967-3334/28/11/005.

[7] K. Arquilla, A.K. Webb, A.P. Anderson, Woven electrocardiogram (ECG) electrodes for health monitoring in operational environments, Proc. Annu. Int. Conf. IEEE Eng. Med. Biol. Soc. EMBS. (2020 (2020)) 4498–4501, https://doi.org/10.1109/EMBC44109.2020.9176478.

[8] B. Babusiak, S. Borik, L. Balogova, Textile electrodes in capacitive signal sensing applications, Meas. J. Int. Meas. Confed. 114 (2018) 69–77, https://doi.org/10.1016/j.measurement.2017.09.024.

[9] S. Khan, L. Lorenzelli, R.S. Dahiya, Technologies for printing sensors and electronics over large flexible substrates: A review, IEEE Sens. J. 15 (6) (2015) 3164–3185, https://doi.org/10.1109/JSEN.2014.2375203.

[10] A.B. Nigusse, B. Malengier, D.A. Mengistie, L. Van Langenhove, A washable silver-printed textile electrode for ECG monitoring, Eng. Proc. 6 (2021) 63, https://doi.org/10.3390/i3s2021dresden-10139.

[11] G. Fytianos, A. Rahdar, G.Z. Kyzas, Nanomaterials in cosmetics: Recent updates, Nanomaterials 10 (2020) 1–16, https://doi.org/10.3390/nano10050979.

[12] N. Rai H. Shaik N. Veerapandi V.S. Nagaraj S. Veena Carbon-based textile dry and flexible electrodes for ECG measurement . P. S., Prabhu N., K. S Advances in Renewable Energy and Electric Vehicles Lecture Notes in Electrical Engineering 767 (2022) Springer, Singapore 37 53 10.1007/978-981-16-1642-6_4.

[13] M.K. Yapici T. Alkhidir Y.A. Samad K. Liao Graphene-clad textile electrodes for electrocardiogram monitoring Sensors Actuators B Chem. 221 2015 1469 1474 10.1016/j.snb.2015.07.111.

[14] A.A. Chlaihawi, B.B. Narakathu, S. Emamian, B.J. Bazuin, M.Z. Atashbar, Development of printed and flexible dry ECG electrodes, Sens. Bio-Sensing Res. 20 (2018) 9–15, https://doi.org/10.1016/j.sbsr.2018.05.001.

[15] L.M. Ferrari, U. Ismailov, J.M. Badier, F. Greco, E. Ismailova, Conducting polymer tattoo electrodes in clinical electro- and magneto-encephalography, NPJ Flex. Electron. 4 (2020) 1–9, https://doi.org/10.1038/s41528-020-0067-z.

[16] J. Alberto, C. Leal, C. Fernandes, P.A. Lopes, H. Paisana, A.T. de Almeida, M. Tavakoli, Fully untethered battery-free biomonitoring electronic tattoo with wireless energy harvesting, Sci. Rep. 10 (2020) 1–11, https://doi.org/10.1038/s41598-020-62097-6.

[17] J. Ferri, R. Llinares Llopis, J. Moreno, J. Vicente Lidón-Roger, E. Garcia-Breijo, An investigation into the fabrication parameters of screen-printed capacitive sensors on e-textiles, Text. Res. J. 90 (15-16) (2020) 1749–1769, https://doi.org/10.1177/0040517519901016.

[18] N. Pilia, C. Nagel, G. Lenis, S. Becker, O. Dössel, A. Loewe, ECGdeli - An open source ECG delineation toolbox for MATLAB, SoftwareX 13 (2021) 1–8, https://doi.org/10.1016/j.softx.2020.100639.

[19] G. Baldazzi, A. Spanu, A. Mascia, G. Viola, A. Bonfiglio, P. Cosseddu, D. Pani, Validation of a novel tattoo electrode for ECG monitoring, Computing in Cardiology 48 (2021) 1–4. https://www.cinc.org/2021/Program/accepted/154_Preprint.pdf.

[20] I.G. Trindade, F. Martins, R. Dias, C. Oliveira, J, Machado Da Silva, Novel textile systems for the continuous monitoring of vital signals: Design and characterization, Proc. Annu. Int. Conf. IEEE Eng. Med. Biol. Soc. EMBS (2015 (2015)) 3743–3746, https://doi.org/10.1109/EMBC.2015.7319207.